VOL. 12, NO. 19, OCTOBER 2017 ISSN 1819-6608
ARPN Journal of Engineering and Applied Sciences

www.arpnjournals.com

ANALYSIS OF HEAT TRANSFER IN TURBULENT FLOW THROUGH THE TUBE WITH UNIFORM HEAT FLUX

Kianoush Dolati Asl[1] and Ahmad Jalali[2]
[1]Department of Mechanical Engineering, Payame Noor University, Tehran, Iran
[2]Department of Mechanical Engineering, Hormozgan University, Bandar Abbas, Iran
E-Mail: kianoush.dolati@gmail.com

ABSTRACT

Turbulent flow and heat transfer in tubes are among the most important issues in almost all industries. This paper aims to numerically analyze forced convective heat transfer within the tube. To this end, the fluid flow in the tube is considered as turbulent together with heat flux along the entire surface of the tube. In this article, the Reynolds number varies in a range of 5273-20, 000. Also, the Prandtl number (Pr) is considered equal to 0.7 and 4 for the target fluid. A non-uniform three-dimensional network along with Spalart-Allmaras turbulence model is used for modeling and simulation of the fluid flow and heat transfer. The length of the tube used in this study is 25 times of its diameter. In this study, after reviewing the validity of the results, changes in the fluid temperature inside the tube are investigated based on the distance from the tube wall and along the length of the tube. Moreover, the tube surface temperature is studied for flows with different Reynolds numbers. Results show that the mean tube surface temperature decreases by increasing the value of the Reynolds number, whereas it increases by increasing the Prandtl number. Moreover, it is observed that, with increasing the Prandtl number, the tube surface temperature is more quickly stabilized.

Keywords: heat transfer, turbulent flow, tube, three-dimensional, heat flux.

INTRODUCTION

In many industrial equipment facilities, heat transfer in the tube sidewall is of great importance, especially in cases where the tube flow is of turbulent type with high temperature gradient and heat transfer rates, such as in heat exchangers, turbines and solar collectors [1-3]. Also, by knowing the principles of fluid flow and heat transfer in tubes with heat flux on the sidewall, physical properties of various types of fluids and nanofluids can be obtained [4-5]. Numerous experimental and numerical works have been carried out to examine properties of the fluid flow and heat transfer through them, the results of some of which have been the proposition of semi-experimental equations [6-8].

Several studies have been presented investigating heat transfer as a function of the Reynolds number and roughness [9-11]. Using the k-ε turbulence model, turbulent fluid flow inside the tube was modelled, which showed a good consistency with the experimental results [12-14]. The turbulent fluid flow was modelled regardless of heat transfer and through using the direct numerical simulation (DNS) [15-16]. Also, heat transfer was investigated as uniform heat flux on the tube sidewall for the turbulent fluid flow through the use of the DNS technique [17-19].

In this study, the turbulent flow inside a 3D tube was investigated using the Spalart-Allmaras turbulent flow model. Also, heat transfer was examined based on the presence of constant and uniform heat flux on the surface of the tube. The schematic form of the tube used in this study is shown in Figure-1. In this study, the properties of the target fluid have been considered constant. Also, the Reynolds number here has values of 5273, 10000, 15000 and 20000. The Prandtl number was considered equal to 0.7 and 4 for the target fluid, which is independent of temperature.

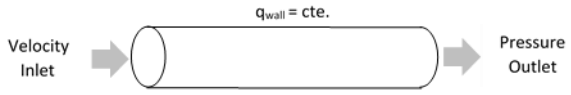

Figure-1. Schematic form of the examined tube.

Mathematical equations

As mentioned in the introduction, heat transfer and turbulent fluid flow inside the tube were examined in this paper. Accordingly, a model must be used with the ability to model fluid flow in the tube sidewall. In general, the continuity equation in differential form is as follows:

$$\frac{\partial \rho}{\partial t} + \nabla.(\rho \vec{v}) = 0 \quad (1)$$

where ρ is the density, t the time and $\vec{v}$ the average velocity at the tube cross section. Momentum conservation equation is as follows:

$$\frac{\partial}{\partial t}(\rho \vec{v}) + \nabla.(\rho \vec{v}\vec{v}) = -\nabla p + \nabla.(\bar{\bar{\tau}}) + \rho \vec{g} + \vec{F} \quad (2)$$

where ∇p is the pressure difference, $\rho \vec{g}$ the gravity, $\bar{\bar{\tau}}$ the stress tensor and $\vec{F}$ the external force.

The Spalart-Allmaras model is a single-equation model which is used to solve the modelled transport equation for eddy viscosity [20]:

$$\frac{\partial}{\partial t}(\rho \tilde{v}) + \frac{\partial}{\partial x_i}(\rho \tilde{v} u_i) = G_v + \frac{1}{\sigma_{\tilde{v}}}\frac{\partial}{\partial x_i}\left[(\mu + \rho \tilde{v})\frac{\partial \tilde{v}}{\partial x_i}\right] + \frac{C_{b2}\rho}{\sigma_{\tilde{v}}}\left(\frac{\partial \tilde{v}}{\partial x_i}\right)^2 - Y_v \quad (3)$$

where G_v is the turbulent viscosity production and Y_v the turbulent viscosity destruction. Also, $\sigma_{\tilde{v}}$ and C_{b2} are equal to 0.667 and 0.622, respectively, and v is the

molecular kinematic viscosity. Turbulent heat transfer is modeled by the following equation:

$$\frac{\partial}{\partial t}(\rho E) + \frac{\partial}{\partial x_i}[u_i(\rho E + p)] = \frac{\partial}{\partial x_i}\left[\left(k + \frac{C_p \mu_t}{Pr_i}\right)\frac{\partial T}{\partial x_i} + u_i(\tau_{ij})_{eff}\right] \quad (4)$$

where k is the thermal conductivity ratio and E the total energy. Here, $(\tau_{ij})_{eff}$ is as follows:

$$(\tau_{ij})_{eff} = \mu_{eff}\left(\frac{\partial u_j}{\partial x_i} + \frac{\partial u_i}{\partial x_j}\right) - \frac{2}{3}\mu_{eff}\frac{\partial u_k}{\partial x_k}\delta_{ij} \quad (5)$$

where the Reynolds number is defined as $Re = \frac{\rho u D}{\mu}$. The temperature difference between the fluid and wall is:

$$\langle T \rangle = T_{(r,\theta)} - T_{wall} \quad (6)$$

where $T_{(r,\theta)}$ is the fluid temperature in different parts of the tube and T_{wall} the tube surface temperature at the desired cross section. Here, the characteristic friction temperature (T^*) is as follows:

$$T^* = \frac{\overline{q_w}}{\rho C_p u_\tau} \quad (7)$$

where $\overline{q_w}$ is the net heat flux on the wall and u_τ the shear rate [21]:

$$u_\tau = \sqrt{\frac{\tau_w}{\rho}} \quad (8)$$

The non-dimensional space inside the tube to the tube wall is:

$$y^+ = \frac{(R-r)u_\tau}{\nu} \quad (9)$$

where R is the tube radius and r the distance of the target point to the tube center.

In this study, the tube length was considered 25 times of its diameter. The tube inlet was considered as 300 K based on the inlet velocity consistent with the fluid temperature. Moreover, steady fluid flow was without the presence of volumetric forces and source of energy supply. On the tube sidewall, no-slip condition was applied.

The generated network has 500 elements along the length of the tube and almost 1250 elements at the tube cross section. The generated network is gathered near the wall and also, near the inlet. It is observed that, with increasing the number of elements, the results do not significantly change. The governing equations are solved by the fluent software and through using the SIMPLE algorithm. Further, Spalart-Allmaras model could be applied in the range of y^+between 1 and 30.

The fluid velocity in the tube inlet was equal to 0.005273, 0.01, 0.015 and 0.02 m/s. Moreover, the fluid Prandtl number was considered as 0.7 and 4, its density value equal to 1000 kilograms per cubic meter and its viscosity equal to 0.001 kg/m.s. Here, $\overline{q_w}$ is constantly and uniformly distributed throughout the tube and its value is equal to 100 watts per square meter.

RESULTS

This section includes analyzing the results related to the topic of fluid flow inside the tube and also, heat transfer existing within the tube. The diagram of the y^+ value on the tube sidewall is shown in Figure-2. It can be seen that the y^+ value is less than 5 across the entire tube length, which indicates the appropriate networking of the issue. However, at the beginning of the tube where the fluid flow is in the inlet length area, y^+had its maximum value.

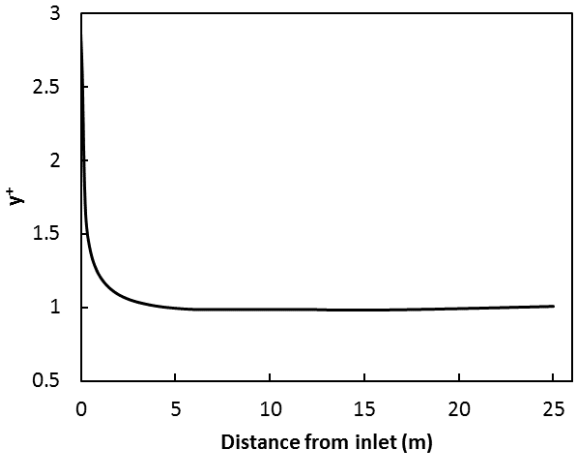

Figure-2. Investigation of the validity of the used network with the non-dimensional space relative to the tube surface.

In Figure-3, comparative diagram of the results obtained for the average shear stress rate across the tube length based on the Reynolds number ranging between 10,000-30, 000 is shown. The results obtained by Ahsan [12] were used to validate the modelling results, which represents a good agreement between the results. Also, Figure-3 shows that, by increasing the Reynolds number, the average shear stress rate also increases across the entire tube length, resulting in the pressure drop throughout the tube length.

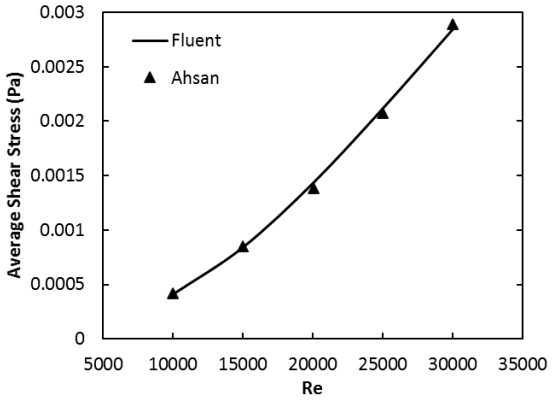

Figure-3. The diagram of changes of the average shear stress on the tube surface relative to the Reynolds number.

In Figure-4, the comparative diagram of the temperature $\langle T \rangle / T^*$ at the tube cross section is shown as a function of the y^+ value. As can be seen in Figure-4, the Reynolds number and Prandtl number are plotted as equal to 5273 and 0.7, respectively. Also, this diagram compared the results obtained in this study and those previously obtained by other researchers. As shown in this diagram, the results obtained in this study are in good agreement with previous results.

As previously shown in the results, the modeling and simulation conducted by the Spalart-Allmaras turbulent flow model have a good ability to obtain results related to fluid flow and heat transfer inside the tube.

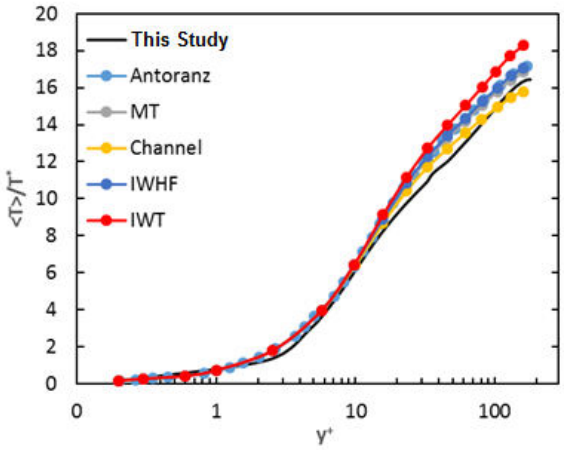

Figure-4. The diagram of the fluid temperature difference with the y^+ radial distance from the tube surface to the tube surface temperature.

Figure-5 shows changes in temperature of the fluid at the tube cross section in terms of radial distance from the tube center. The fluid flows examined in Figure-5 have the Reynolds number ranging between 5273 and 20,000. Also, the Prandtl number of the fluid examined here is equal to 0.7.

As shown in Figure-5, by increasing the Reynolds number and subsequently, increasing the fluid mass flow rate, the tube wall temperature is reduced. Furthermore, it is observed in this diagram that the bulk of tube cross section is covered with a fluid with uniform temperature, and the only section located within the radial distance of almost less than 0.05 m from the wall is experiencing a sharp temperature gradient. One of the causes of such sharp temperature gradient near the wall is the existence of the boundary layer and radial velocity component near the wall that lead to the transfer of momentum and heat. According to Fourier's law of heat conduction, such a sharp temperature gradient causes increased heat conduction in the layer near the wall and thus, the temperature gradient increases in this area due to the presence of two types of heat conduction and displacement.

Figure-6 shows the changes in the fluid temperature difference with the distance r from the center of the tube and the tube surface temperature, in non-dimensional form, with $T^*$for the fluid with $Pr = 0.7$. It is observed that the $\langle T \rangle / T^*$ values are very close together in high Reynolds numbers. As shown in Figure-6, the highest temperature gradient exists near the tube wall, and the fluid temperature gradient is lower that the layer close to the tube wall in almost all the areas at the tube cross section.

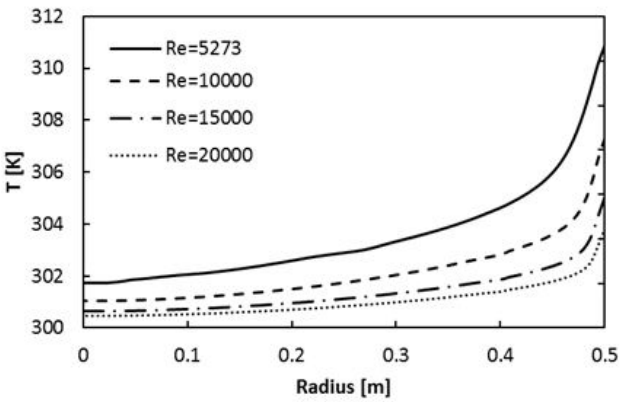

Figure-5. The fluid temperature changes along the tube radius.

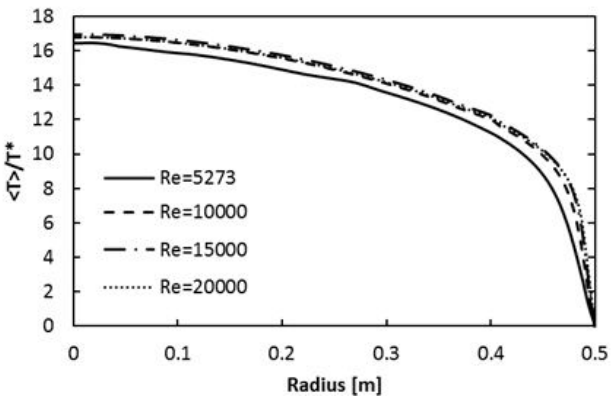

Figure-6. Changes of the fluid temperature to the tube surface along the tube radius and with the distance r from the tube center in the non-dimensional form ($Pr = 0.7$).

Figures 7 to 10 show how temperature changes along the length of the tube for 3 modes of $r = 0$, $r = R/2$ and $r = R$. The static temperature along the tube center and with the distance R from the center of the tube is shown as a continuous line. The $\langle T \rangle / T^*$ temperature value, where $\langle T \rangle$ is calculated at the same cross section based on the temperature difference between the fluid and tube surface, is plotted for the fluid at the tube center (two dotted line) and also at the radial distance $R/2$ from the tube center (dashed line). The Prandtl number intended for the fluid is $Pr = 0.7$.

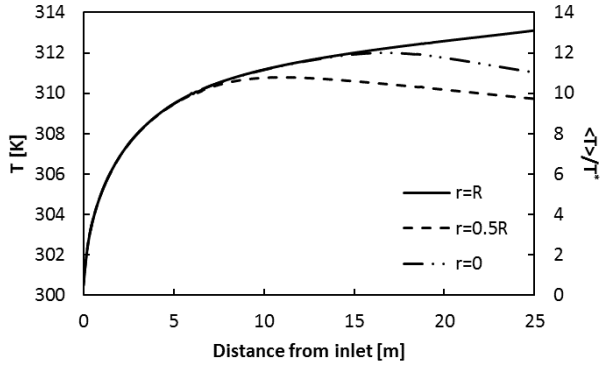

Figure-7. Temperature changes along the length of the tube for the Reynolds equal to 5273.

As shown in Figures 7 to 10, by increasing the Reynolds number, the end temperature of the tube surface is reduced due to further volumetric flow rate of the inlet fluid. Constant heat flux on the tube surface and increased inlet flow rate, the fluid temperature inside the tube is reduced.

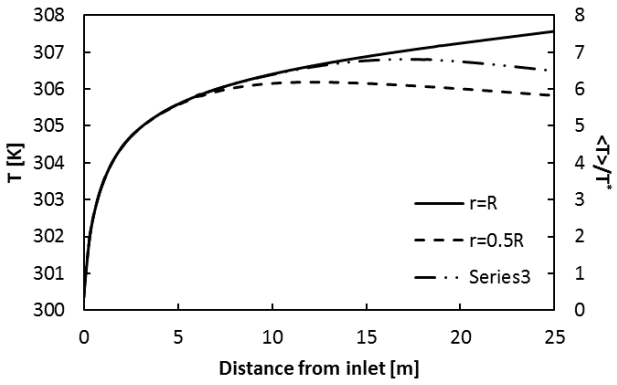

Figure-8. Temperature changes along the length of the tube for the Reynolds equal to 10000.

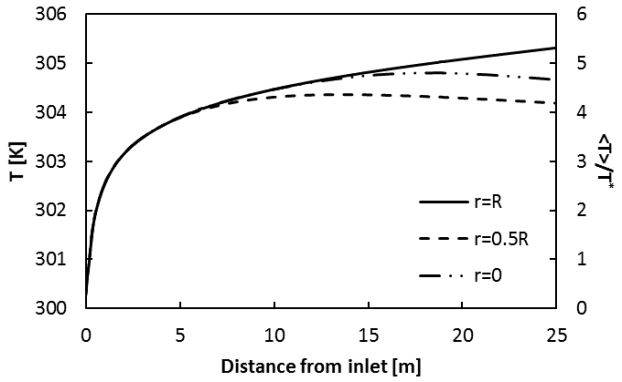

Figure-9. Temperature changes along the length of the tube for the Reynolds equal to 15000.

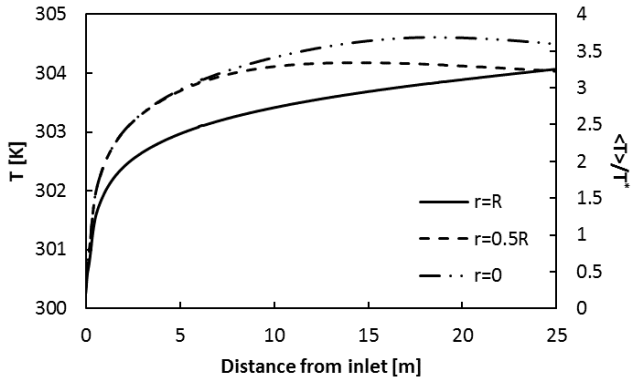

Figure-10. Temperature changes along the length of the tube for the Reynolds equal to 20000.

Moreover, Figures 7 to 10 show that the temperature difference between the fluid inside the tube and the fluid on the tube surface decreases by increasing the Reynolds number. Because, as noted above, the tube surface fluid temperature decreases with increasing the Reynolds number, which leads to reduced temperature difference between the fluid inside the tube and the fluid on the tube surface.

The heat transfer within the tube exists in two forms of conduction heat transfer within the fluid and convection heat transfer due to the presence of radial velocity in the turbulent fluid flow.

As shown in Figures 7 to 10, difference between the fluid temperature inside the tube and the tube surface temperature is on the rise after entering into the tube to a distance of 5 or 6 meters, indicating a sharp rise in the tube surface temperature. However, the temperature of the fluid inside the tube also slightly increases, which is due to conduction heat transfer within the fluid. After about 7 meters from the tube inlet, despite an increase in the tube surface temperature, the difference between the fluid temperature inside the tube and the tube surface temperature decreases. This is because heat transfer exists due to the presence of radial velocity, since with increasing distance from the inlet, the boundary layer

within the tube is also extended, leading to greater radial velocity.

It is seen in Figures 7 to 10 that the difference between the fluid temperature inside the tube and the tube surface temperature faster declines in case the fluid is in the radial distance equal to $R/2$ from the center, as compared to the fluid at the tube center, which is due to faster placement of the radial distance $R/2$ within the fluid boundary layer and consequently, increased heat transfer.

Figures 11 and 12 show the tube surface temperature based on the distance from the inlet to have Prandtl numbers equal to 0.7 and 4 for fluid flows. It is observed that the tube surface temperature gradually decreases with increasing the Reynolds number. Also, the maximum tube surface gradient is at the initial part of the tube, after which the tube surface temperature is almost uniform. By increasing the Reynolds number in flows at low Reynolds numbers, the tube surface temperature is greater reduced than in the condition with high Reynolds number.

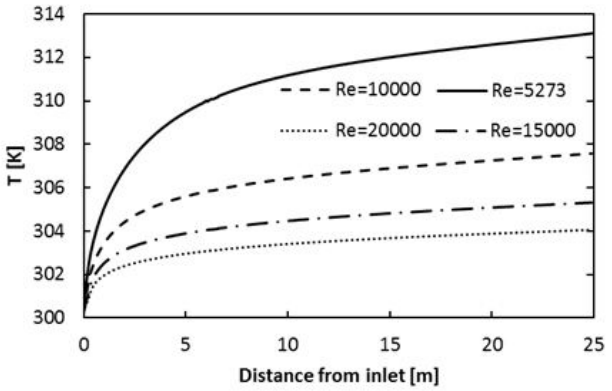

Figure-11. The tube surface temperature changes along the length of the tube ($Pr = 0.7$).

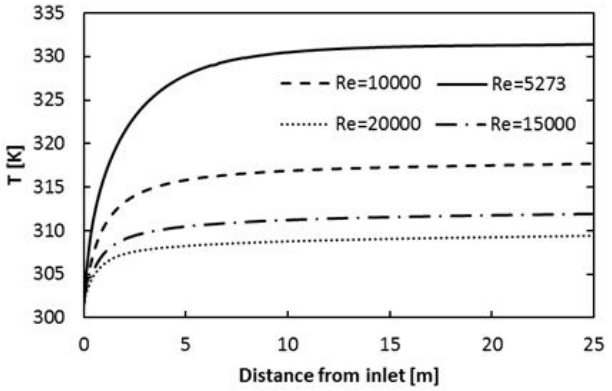

Figure-12. The tube surface temperature changes along the length of the tube ($Pr = 4$).

Also, by comparing Figures 11 and 12, it can be observed that with increasing the Prandtl number, the tube surface temperature reaches the steady state at a lower distance from the inlet. Moreover, increased Prandtl number leads to increased average tube surface temperature. The reason for the increased tube surface temperature with increasing the Prandtl number is that, by increasing the Prandtl number, conduction heat transfer within the fluid decreases due to increased thermal conductivity resistance, and heat within the fluid is concentrated near the wall, as shown in Figures 13 and 14.

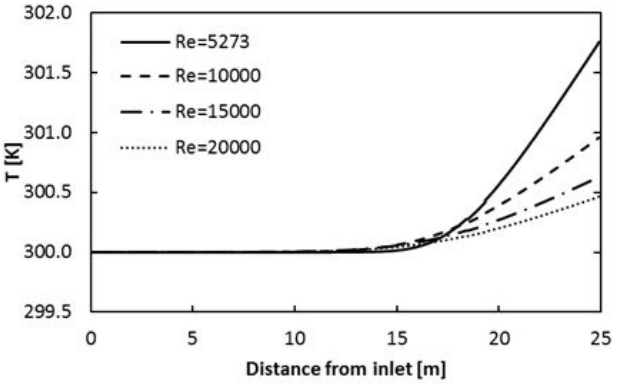

Figure-13. The fluid temperature changes at the tube center and along the tube length ($Pr = 4$).

Figure-13 show the fluid temperature changes along the length of the tube and at its center for the fluid flow with the Prandtl number equal to 4. It is observed that at almost the entire length of the tube and at its center, the fluid temperature equals the temperature of the fluid at the time of entering into the tube and also, the fluid temperature increases near the tube outlet due to insignificant heat transfer rate as a result of high Prandtl number.

Figure-14 shows changes in difference between the fluid temperature at the distance r from the tube center and the tube surface temperature in the non-dimensional from with T^* for the fluid with $Pr = 4$. By comparing Figures 6 and 14, it can be seen that as the Prandtl number increases, the fluid temperature difference rate with the wall surface also increases. Moreover, with increasing the Prandtl number, the temperature gradient becomes more severe near the tube wall, and the fluid temperature is uniform across most parts of the tube cross section. For flows with Reynolds numbers of 15,000 and 20,000, diagrams of difference between the fluid temperature inside the tube and the tube surface temperature almost overlap.

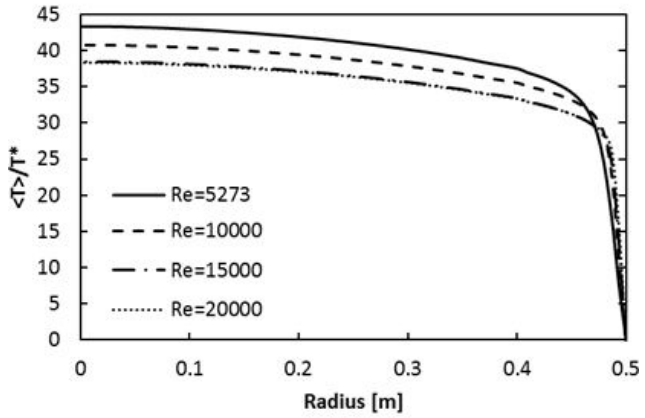

Figure-14. The fluid temperature changes relative to the tube surface along the tube radius and at the distance r from the tube center in the non-dimensional form ($Pr = 4$).

The average value of the Nusselt number across the tube for various fluid flows is shown in Table-1. It is observed that in the fixed Reynolds number condition, increasing the Prandtl number causes the Nusselt number to increase. Also, in case the Prandtl number has a fixed value, the Nusselt number increases by increasing the Reynolds number.

Table-1. Nusselt number at tube surface.

Reynolds Number	5273	10000	15000	20000
Nusselt (Pr=0.7)	17.359	28.976	40.99	53.118
Nusselt (Pr=4)	37.526	64.665	94.827	119.431

Figures 15 and 16 plot the diagram of changes in the Nusselt number for the fluid with the Prandtl numbers of 0.7 and 4. As can be seen, the Nusselt number severely changes at the tube inlet, but the change is greatly reduced after passing some distance within the tube. Moreover, by increasing the Reynolds number, the value of the Nusselt number and consequently, the heat transfer value increases.

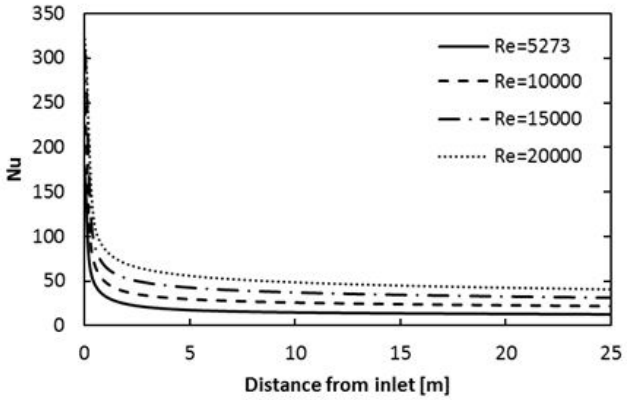

Figure-15. The Nusselt number for the fluid flow at $Pr = 0.7$.

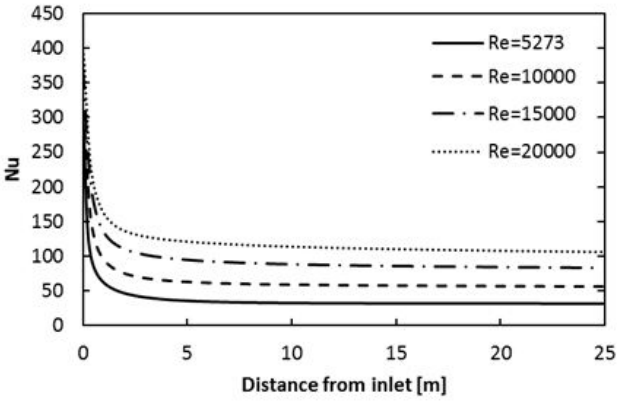

Figure-16. The Nusselt number for the fluid flow at $Pr = 4$.

By comparing the results in Table-1 and those in Figures 15 and 16, it can be concluded that in almost the entire tube length, the Nusselt number has a lower value than its average value, and the highest Nusselt number value exists at the tube inlet. Further, by comparing Figures 15 and 16, it is seen that the Nusselt number value increased with increasing the Prandtl number.

CONCLUSIONS

In this study, the heat transfer within the tube with turbulent flow along with constant heat flux at the tube wall was evaluated. To this end, the Prandtl number of the fluid used here was equal to 0.7 and 4 and also, the Reynolds number for the fluid flow was considered as varying between 5273 and 20,000. First, for the purpose of validation of the modeling and simulation, some results obtained in this study were compared with data from other researchers.

It was observed that with increasing the Reynolds number, the outlet fluid temperature was more uniform at different radial distances from the tube center, which becomes more severe in case the Prandtl number increases. Moreover, the highest temperature gradient existing at the cross section of the tube was observed near the tube wall, which is regarded as a small area compared

to the overall tube surface. By increasing the Reynolds number, the fluid temperature difference was reduced, as compared to the tube surface, along the tube radius and at the distance r from the center of the tube.

The results also revealed that the highest proportion for the heat transfer to the fluid flowing at the tube center belonged to convection heat transfer, and the proportion of conduction heat transfer within the fluid decreased by increasing the Prandtl number. Moreover, by increasing the Reynolds number, the average tube surface temperature was observed to decrease. Also, the tube surface temperature was seen to become more uniform and greater in the average value with increasing the Prandtl number.

According to the results, the fluid on the central line of the tube traveled up to 60% of the tube length without any altered temperature, and the temperature only began to increase after this distance up to the tube outlet. At the tube inlet, the Nusselt number was observed to be extremely high in value; however, within the following 90% of the tube length, the Nusselt number had a lower value than the average. Also, it was found that, with increasing the Reynolds or Prandtl number, the Nusselt number also increased. However, the effect of the increased Reynolds number on the Nusselt number was realized to be higher in flows having fluids with high Prandtl number.

REFERENCES

[1] Aly A. 2014. Atmospheric boundary-layer simulation for the built environment: past, present and future. Build Environ. 75: 206-221.

[2] Aly A. and Bitsuamlak G. 2013. Aerodynamics of ground-mounted solar panels: test model scale effects. Journal of Wind Engineering and Industrial Aerodynamics. 123: 250-260.

[3] Kolb G.J. 2011. An evaluation of possible next-generation high-temperature molten-salt power towers. Sandia National Labs.

[4] Kristiawan B., Kamal S. and Yanuar 2015. Convective heat transfer of titanium (IV) oxide nanofluids under turbulent flow condition. ARPN Journal of Engineering and Applied Sciences. 10(10): 4385-4395.

[5] Abdul Hamid K., Azmi W.H., Mamat R., Usri N.A. and Najafi G. 2015. Effect of titanium oxide nano-fluid concentration on pressure drop. ARPN Journal of Engineering and Applied Sciences. 10(17): 7815-7820.

[6] Bejan A. 2013. Convection Heat Transfer. John Wiley & Sons, Inc.

[7] Dittus F.W. and Boelter L.M.K. 1985. Heat transfer in automobile radiators of the tubular tube. International Communications in Heat and Mass Transfer. 12(1): 3-22.

[8] Gnielinski V. 1976. New equations for heat and mass transfer in turbulent pipe and channel flow. International Chemical Engineering. 16: 359-368.

[9] Fabbri G. 2000. Heat transfer optimization in corrugated wall channels. International Journal of Heat Mass Transfer. 43(23): 4299-4310.

[10] Togun H., Kazi S. and Badarudin A. 2011. A review of experimental study of turbulent heat transfer in separated flow. Australian Journal of Basic and Applied Sciences. 5(10): 489-505.

[11] Zhang Z., Lowe R., Falter J. and Ivey G. 2011. A numerical model of wave-and current-driven nutrient uptake by coral reef communities. Ecological Modelling. 222(8): 1456-1470.

[12] Ahsan M. 2014. Numerical analysis of friction factor for a fully developed turbulent flow using k-ε turbulence model with enhanced wall treatment. beni-suef university journal of basic and applied sciences. 3: 269-277.

[13] Di Nucci C. and Russo Spena A. 2012. Mean velocity profiles of two dimensional fully developed turbulent flows. Comptes Rendus Mécanique. 340(9): 629-640.

[14] Cardwell N.D., Vlachos P.P. and Thole K.A. 2011. Developing and fully developed turbulent flow in ribbed channels. Experiments in Fluids. 50(5): 1357-1371.

[15] El Khoury G., Schlatter P., Noorani A., Fischer P., Brethouwer G. and Johansson A. 2013. Direct numerical simulation of turbulent pipe flow at moderately high Reynolds numbers. Flow, Turbulence and Combustion. 91: 475-495.

[16] Wu X. and Moin P. 2008. A direct numerical simulation study on the mean velocity characteristics in turbulent pipe flow. Journal of Fluid Mechanics. 608: 81-112.

[17] Antoranz A., Gonzalo A., Flores O. and García-Villalba M. 2015. Numerical simulation of heat transfer in a pipe with non-homogeneous thermal boundary conditions. International Journal of Heat and Fluid Flow. 55: 45-51.

[18] Chin C., Monty J. and Ooi A. 2014. Reynolds number effects in DNS of pipe flow and comparison with channels and boundary layers. International Journal of Heat Fluid Flow. 45: 33-40.

[19] Redjem-Saad L., Ould-Rouiss M. and Lauriat D. 2007. Direct numerical simulation of turbulent heat transfer in pipe flows: effect of Prandtl number. International Journal of Heat Fluid Flow. 28: 847-861.

[20] Spalart P. and Allmaras S. 1992. A one-equation turbulence model for aerodynamic flows. American Institute of Aeronautics and Astronautics.

[21] Piller M. 2005. Direct numerical simulation of turbulent forced convection in awavy channel at low and order one Prandtl number. International Journal for Numerical Methods in Fluids. 49: 583-602.